# ST3Gal1 modulates intestinal barrier function and impacts human ulcerative colitis

YIN TIAN[1], YUN LIU[2], YANGYANG SHANG[2], LIJIAN RAN[2], LI LIU[2], RONGQUAN WANG[2] and JUN YE[2]

[1]Department of Gastroenterology, The People's Hospital of Yubei District of Chongqing City, Chongqing 401120, P.R. China; [2]Institute of Gastroenterology of People's Liberation Army, Southwest Hospital, Army Medical University, Chongqing 400038, P.R. China

Received October 17, 2025; Accepted December 12, 2025

DOI: 10.3892/mmr.2025.13783

**Abstract.** The pathogenesis of inflammatory bowel disease is associated with dysfunction of the intestinal mucosal barrier. Protein sialylation serves an important role in maintaining the integrity of this barrier. The present study investigated how α2,3-linked sialylation catalyzed by protein ST3Gal1 affected intestinal barrier function and impacted the pathogenesis of human ulcerative colitis (UC). The present study employed Caco-2, HT29-MTX-E12 and THP-1 cells with distinct functionalities to establish an *in vitro* triple-culture model. This model was utilized to simulate both healthy and inflamed states of the human intestine for investigating the impact of ST3Gal1-mediated α2,3-sialylation on the integrity of the intestinal barrier. The triple-culture model was stably infected with adenoviral particles or lentiviral vectors to establish ST3Gal1 knockdown and overexpression, respectively, followed by isolation through incubation with 4 $\mu$g/ml puromycin. The functionality of the intestinal barrier was assessed via trans-epithelial electrical resistance and FITC-dextran permeability assays. ST3Gal1 expression was found to be associated with inflammation of the intestinal mucosa in patients with UC and a mouse model of dextran sulfate sodium-induced colitis. Notably, suppressed expression of ST3Gal1 in the intestinal epithelial cell (IEC) monolayer enhanced the functionality of the intestinal barrier, whereas its overexpression caused intestinal barrier function deterioration. ST3Gal1 expression in the IEC monolayer altered the expression of intestinal mucus barrier-associated mucin 2 (MUC2) and trefoil factor 3 (TFF3), goblet cell differentiation-associated homeobox protein CDX-2 (CDX2), inflammation-associated phosphorylated (p)-STAT3, and the inflammatory mediators IL-1β, IL-6 and IL-8. Specifically, MUC2, TFF3 and CDX2 were positively associated with enhanced barrier integrity, whereas p-STAT3, IL-1β, IL-6 and IL-8 were negatively correlated with barrier function. Collectively, these results demonstrated a strong association between these factors and the regulation of intestinal barrier function. In conclusion, ST3Gal1-catalyzed α2,3-linkage formation in IECs may be closely associated with intestinal barrier function via its effect on the expression of barrier-associated proteins and inflammatory mediators related to intestinal mucosa inflammation.

*Correspondence to:* Professor Rongquan Wang or Professor Jun Ye, Institute of Gastroenterology of People's Liberation Army, Southwest Hospital, Army Medical University, 30 Gaotanyan Zhengjie, Shapingba, Chongqing 400038, P.R. China
E-mail: wangrongquan@tmmu.edu.cn
E-mail: yejun@tmmu.edu.cn

*Key words:* sialylation, barrier, inflammation, ST3Gal1, triple culture model

## Introduction

Inflammatory bowel diseases (IBDs) comprise chronic as well as recurrent gastrointestinal conditions. A recent study has reported on the notable increase in the global prevalence of IBD, predominantly characterized by Crohn's disease (CD) and ulcerative colitis (UC) (1). Impaired intestinal barrier integrity is a contributing factor in the pathogenesis of IBD and is closely associated with its pathophysiology (2,3). Despite this, there is a characteristic lack of therapeutic options that specifically enhance mucosal barrier function and promote its regeneration in IBD, which is likely owing to a limited understanding of the underlying biological pathways and regulatory molecules involved (4). Although various potential therapeutic approaches have been developed for improving mucosal barrier function (4,5), to the best of our knowledge, no regenerative strategies have yet been developed specifically for IBD.

Glycosylation is a post-translational modification affecting proteins, lipids and RNA, which can profoundly influence the structural and functional characteristics of the modified molecules (6-8). This modification is important for regulating a variety of biological mechanisms, including protein maturation, transport and immune modulation (9). Glycosylation is also implicated in the pathophysiology of severe diseases, such as during carcinogenesis, and inflammation; a previous study also demonstrated its association with IBD (10). In healthy individuals, protein glycoforms exhibit substantial stability over time; however, they tend to undergo notable alterations in response to pathological conditions, particularly during inflammatory states. For example, patients diagnosed with IBD exhibit increased expression levels of short-chain O-glycans in the intestine compared with healthy individuals, accompanied

by alterations in the expression of terminal glycan structures (for example, increased sialylation, enhanced fucosylation, reduced sulfation and dysregulated Lewis antigens). These changes adversely affect the integrity of the intestinal mucus layer, impede glycan-lectin interactions, disrupt the dynamic balance of the intestinal microbiota and impair the functionality of the intestinal mucosal immune system (11).

Different sialylation modifications are catalyzed by various sialyltransferases. However, any alterations in the expression levels of sialyltransferases change their physiological functions. For example, a decrease in sialyltransferase ST6GalNAc1 (ST6)-catalyzed α2,6-sialylation in mice results in impaired mucus barrier function, gut microbiota dysbiosis and increased susceptibility to intestinal inflammation (12). The α2,6-sialylation catalyzed by ST6Gal1 promotes the activation of $CD4^+$ T cells and induces the development of UC (13), whereas α2,8-sialylation catalyzed by ST8Sia4 facilitates the metastasis of breast cancer cells (14). However, the role of ST3Gal1-catalyzed α2,3-sialylation in intestinal inflammation remains to be fully elucidated.

The upregulation of ST3Gal1 augments the sialylation of O-glycan Tn and catalyzes its conversion into sialyl-Tn. This modification introduces an α2,3-linkage between Gal and β1,3-GalNAc, which is frequently observed in various cancer types, including breast cancer and hematological malignancies, where the upregulation of sialyltransferases leads to premature termination of aberrant mucin-type O-glycan chains (15,16). Notably, mucin-type O-linked glycosylation is not restricted to mucins; this modification also occurs in an array of cell-surface glycoproteins (17). Emerging evidence has highlighted that glycosylation in intestinal epithelial cells (IECs) is associated with specific glycosyltransferases; however, the functional role of ST3Gal1-catalyzed α2,3-sialylation, a key glycosylation event mediated by this glycosyltransferase, in the regulation of intestinal barrier function has often been neglected in relevant research. Dysregulation of glycosylation exacerbates intestinal inflammation by damaging the intestinal barrier integrity, interfering with glycan-lectin interactions, disrupting intestinal microbiota dynamics and impairing mucosal immunity (18-20).

Given that ST3Gal1-catalyzed α2,3-linkage formation at the end of N-glycan or O-glycan is associated with carcinogenesis, as well as a host of other diseases, it is necessary to evaluate prognostic factors, identify predictive biomarkers and explore possible therapeutic targets associated with ST3Gal1 activity, particularly in IBD (15,21). However, there is limited research on ST3Gal1 and its impact on the function of the intestinal barrier.

The present study aimed to explore the potential role of ST3Gal1-catalyzed α2,3-linkage in IBD, along with its underlying mechanisms. The present experimental study employed an *in vitro* triple-cell co-culture system to replicate both the healthy and inflamed states of the human intestine to investigate the impact of ST3Gal1-mediated α2,3-sialylation on the integrity of intestinal mucosal barrier function. Notably, in the present model, each cell type embodied distinct roles: i) Caco-2 cells formed a monolayer that mimicked IECs; ii) HT29-MTX-E12 cells secreted mucus and acted as a surrogate for intestinal goblet cells; and iii) THP-1 cells, upon induction with phorbol 12-myristate 13-acetate (PMA), differentiated into macrophage-like cells, simulating intestinal inflammatory cells (22-24). The present model adhered to the principles of the 3R framework, which are replacement, reduction and refinement of animal model usage, thus underscoring the increasing importance of *in vitro* models in intestinal health research (25).

## Materials and methods

*Cell culture*. The colorectal cancer cell line HT-29-MTX was sourced from Beijing Bohui Innovation Biotechnology Co., Ltd., whereas the THP-1 human monocytic leukemia and Caco-2 human colorectal adenocarcinoma cell lines were obtained from The Cell Bank of Type Culture Collection of The Chinese Academy of Sciences. All cells were authenticated by short tandem repeat profiling and were cultured in RPMI-1640 medium (Merck KGaA) supplemented with 10% heat-inactivated fetal bovine serum (HyClone™; Cytiva). Cell cultures were maintained in a humidified incubator at 37˚C with 5% $CO_2$.

*Cell culture model*. To establish an IEC monolayer, Caco-2 and HT29-MTX-E12 cells were co-seeded at a total density of $8x10^4$ cells/well into the apical compartment of 24-well Transwell inserts (pore size, 0.4 $\mu$m; Wuxi NEST Biotechnology Co., Ltd.) at a ratio of 9:1, based on this ratio and total cell density, the seeding number of Caco-2 cells was $7.2x10^4$ cells/well, and that of HT29-MTX-E12 cells was $8x10^3$ cells/well, followed by a differentiation period of 19 days. Concurrently, the culture medium was replaced three times a week to maintain optimal growth conditions. Additionally, THP-1 cells were stimulated to differentiate into macrophage-like cells by applying PMA (100 ng/ml; Beyotime Biotechnology) at 37˚C with 5% $CO_2$ for 48 h in 24-well plates. Subsequently, the differentiated macrophage-like THP-1 cells were cultured in the basolateral compartment of the same Transwell plate. The IEC monolayer and macrophage-like THP-1 cells were co-cultured for 24 h under standard conditions (37˚C, 5% $CO_2$) to simulate the intestinal mucosa *in vitro*.

*ST3Gal1 overexpression (ST3Gal1-OE) assay*. Lentiviral vectors designed for the overexpression of ST3Gal1 were procured from Shanghai GenePharma Co., Ltd. The ST3Gal1-OE lentiviral vector was constructed using the LV5(EF-1α/CopGFP&Puro) backbone, based on the 3rd-generation lentiviral system, with a working concentration of $1x10^{10}$ plaque-forming units (PFU)/ml. The lentiviral particles were produced by transfecting 293T cells (American Type Culture Collection). For transfection, a total of 10 $\mu$g plasmids was used, and the molar ratio of lentiviral expression plasmid (ST3Gal1-OE)/packaging plasmid/envelope plasmid was 4:3:1. The transfection was performed using Lipofectamine® 3000 Transfection Reagent (Invitrogen; Thermo Fisher Scientific, Inc.) according to the manufacturer's instructions, under the conditions of 37˚C and 5% $CO_2$ for a duration of 48 h to facilitate lentivirus production. The negative control for overexpression experiments was an empty LV5 vector (Shanghai GenePharma Co., Ltd.), used at the same concentration ($1x10^{10}$ PFU/ml).

Following the precise guidelines set forth by the manufacturer, infection of the cells in the triple co-culture model was performed within the Transwell system, with lentiviral vectors added to both the upper and lower chambers. For lentiviral transduction, polybrene (Shanghai GenePharma Co., Ltd.) was added to the culture medium at a final concentration of 5 $\mu$g/ml to enhance infection efficiency, and the lentiviral particles were used at a multiplicity of infection of 10. The infected cells were then incubated at 37˚C for 24 h. Subsequently, 4 $\mu$g/ml puromycin (MilliporeSigma; Merck KGaA) was used for the initial selection of stably infected cell lines for 7 days, followed by maintenance with 2 $\mu$g/ml puromycin thereafter. These cell lines were subsequently classified as OE-Ctr/IEC (negative control group) and ST3Gal1-OE/IEC groups. Cells were collected on day 9 post-infection (after the completion of the 1-day infection plus a 7-day selection process), and the successful overexpression of ST3Gal1 was confirmed through reverse transcription-quantitative PCR (RT-qPCR) and western blot analysis.

*ST3Gal1 interference assay*. Adenoviral particles designed for interfering with the ST3Gal1 enzyme were obtained from Shanghai GenePharma Co., Ltd. The adenoviral constructs were based on the ADV1(U6/CMV-GFP) vector (2nd-generation adenoviral expression system), which separately harbored three distinct ST3Gal1-targeting short hairpin RNA (shRNA; ST3Gal1-sh) inserts or a non-targeting scrambled negative control shRNA (sh-Ctr). The specific interference target sequences and full-length sense/antisense shRNA fragments were as follows: ST3Gal1 sh1, target sequence 5'-GCACCATTTCCCACACCTACA-3', sense strand'-AATTCGCACCATTTCCCACACCTACATTCAAGAGATGTAGGTGTGGGAAATGGTGCTTTTTTG-3', antisense strand 5'-GATCCAAAAAAGCACCATTTCCCACACCTACATCTCTTGAATGTAGGTGTGGGAAATGGTGCG-3'; ST3Gal1 sh2, target sequence 5'-GCATCCTCTCGGTCATCTTCT-3', sense strand 5'-AATTCGCATCCTCTCGGTCATCTTCTTTCAAGAGAAGAAGATGACCGAGAGGATGCTTTTTTG-3', antisense strand 5'-GATCCAAAAAAGCATCCTCTCGGTCATCTTCTTCTCTTGAAAGAAGATGACCGAGAGGATGCG-3'; ST3Gal1 sh3, target sequence 5'-GGTTCGATGAGAGGTTCAACC-3', sense strand 5'-AATTCGGTTCGATGAGAGGTTCAACCTTCAAGAGAGGTTGAACCTCTCATCGAACCTTTTTTG-3', antisense strand 5'-GATCCAAAAAAGGTTCGATGAGAGGTTCAACCCTCTCTTGAAGGTTGAACCTCTCATCGAACCG-3'; and sh-Ctr, target sequence 5'-GTTCTCCGAACGTGTCACGT-3', sense strand 5'-GATCCGTTCTCCGAACGTGTCACGTTTCAAGAGAACGTGACACGTTCGGAGAACTTTTTTG-3', antisense strand 5'-AATTCAAAAAAGTTCTCCGAACGTGTCACGTTCTCTTGAAACGTGACACGTTCGGAGAACG-3'. The adenoviral particles were produced by transfecting 293T cells. For transfection, 10 $\mu$g plasmids were used per 10-cm culture dish, and the molar ratio of adenoviral expression plasmid (ST3Gal1-sh or sh-Ctr)/packaging plasmid/envelope plasmid was 1:1:1. The transfection was performed using Lipofectamine 3000 Transfection Reagent, according to the manufacturer's instructions, at 37˚C in a humidified atmosphere containing 5% $CO_2$ for 48 h before collecting the adenoviral supernatant.

The triple co-culture cells cultured within the Transwell system were infected with these adenoviral particles in accordance with the manufacturer's guidelines, with adenoviral particles added to both the upper and lower chambers of the Transwell system. The infection procedure was consistent with that used for the infection of overexpression lentiviral vectors aforementioned. These cell lines were subsequently classified as sh-Ctr/IEC and ST3Gal1-sh/IEC groups. The working concentration of adenovirus particles carrying interfering fragments was $1x10^{10}$ PFU/ml, and that of negative control adenovirus particles was $1x10^{10}$ PFU/ml. For adenoviral infection, the MOI was set at 40. Specifically, cells were collected at 48 h post-infection, and the efficiency of the interference was assessed through RT-qPCR and western blot analysis.

*Induction of inflammation in the IEC monolayer*. To establish an *in vitro* UC cell model, ST3Gal1-sh/IEC or ST3Gal1-OE/IEC and their controls were treated with 2% DSS (MilliporeSigma) and incubated in a cell culture incubator at 37˚C for 4 days (26,27). The supernatants were collected by centrifuging the cell cultures at 3,000 x g and 4˚C for 10 min, and were employed for subsequent experiments.

*RT-qPCR*. RNA was isolated and PCR was carried out following the methodologies detailed in our earlier study (28). Briefly, total RNA was extracted from triple co-culture cells, including ST3Gal1-sh, ST3Gal1-OE and their respective negative control cells, using the RNA Isolation Kit (MilliporeSigma; Merck KGaA). RNA purity was assessed by evaluating the A260/A280 ratio (1.8-2.0) with a NanoDrop 2000 spectrophotometer (Thermo Fisher Scientific, Inc.). RNA integrity was verified through 1% agarose gel electrophoresis and by using an Agilent 2100 Bioanalyzer (Agilent Technologies, Inc.), obtaining an RNA integrity number >8.0. cDNA synthesis was performed using the PrimeScript™ RT Reagent Kit with gDNA Eraser (Takara Bio Inc., Japan), according to the manufacturer's protocol. For qPCR, the SYBR® Green Premix Pro Taq HS qPCR Kit (Hunan Accurate Biotechnology Co., Ltd.) was used, with SYBR Green as the PCR fluorophore. Thermocycling conditions were as follows: Pre-denaturation at 95˚C for 3 min, followed by 40 cycles at 95˚C for 30 sec and 60˚C for 30 sec. β-actin was used as the internal reference gene for normalization. Quantification of the qPCR results was performed using the $2^{-\Delta\Delta Cq}$ method (29), and result analysis was performed using Bio-Rad CFX Manager software (version 3.1; Bio-Rad Laboratories, Inc.). Table I displays the sequences of PCR primers utilized in the present experimental investigation.

*Western blotting*. The procedures for protein extraction and detection were carried out in accordance with the methodologies outlined in our previous publication (26). Briefly, total protein was isolated from the triple co-culture cells, including ST3Gal1-sh cells, ST3Gal1-OE cells and their corresponding negative control cells. Table II presents the information regarding the manufacturer, cat. no. and dilution ratios for the primary and secondary antibodies utilized in the present study.

*ELISA*. Cell culture supernatants from each group were collected by centrifuging the cell cultures at 3,000 x g and 4˚C for 10 min. The levels of multiple inflammatory mediators, such as IL-1β, IL-6

Table I. Primer sequences used in reverse transcription-quantitative PCR.

| Primer | Sequence | Product length, bp |
|---|---|---|
| ST3Gal1 | | 74 |
| Forward | 5'-TTCCGGGAGCTGGGAGATAA-3' | |
| Reverse | 5'-CTCACCACCCACTCCAAGTC-3' | |
| MUC2 | | 165 |
| Forward | 5'-GGGGAGTGCTGTAAGAAGTGTGA-3' | |
| Reverse | 5'-GTTGGAGACGGACGAGATGAG-3' | |
| TFF3 | | 143 |
| Forward | 5'-CTCCAGCTCTGCTGAGGAGT-3' | |
| Reverse | 5'-CAGGGATCCTGGAGTCAAAG-3' | |
| CDX2 | | 85 |
| Forward | 5'-CAGGACGAAAGACAAATATC-3' | |
| Reverse | 5'-GATGTAGCGACTGTAGTG-3' | |
| β-actin | | 132 |
| Forward | 5'-GTGATCTCCTTCTGCATCCTGT-3' | |
| Reverse | 5'-CCACGAAACTACCTTCAACTCC-3' | |
| IL-1β | | 153 |
| Forward | 5'-CAGAAGTACCTGAGCTCGCC-3' | |
| Reverse | 5'-AGATTCGTAGCTGGATGCCG-3' | |
| IL-6 | | 166 |
| Forward | 5'-TACCCCCAGGAGAAGATTCC-3' | |
| Reverse | 5'-AGTGCCTCTTTGCTGCTTTC-3' | |
| IL-8 | | 210 |
| Forward | 5'-GTGCAGTTTTGCCAAGGAGT-3' | |
| Reverse | 5'-ACTTCTCCACAACCCTCTGC-3' | |
| STAT3 | | 237 |
| Forward | 5'-CATCCTGAAGCTGACCCAGG-3' | |
| Reverse | 5'-TCCTCACATGGGGGAGGTAG-3' | |

MUC2, mucin 2; TFF3, trefoil factor 3; CDX2, homeobox protein CDX-2.

and IL-8, present in the harvested cell supernatants were measured in accordance with the instructions outlined in the ELISA kits specific to these inflammatory factors (Beijing Solarbio Science & Technology Co., Ltd.): IL-1β (cat. no. SEKH-0002), IL-6 (cat. no. SEKH-0013), and IL-8 (cat. no. SEKH-0016).

*Trans-epithelial electrical resistance (TEER) assay*. Cells from each group were plated at a density of $1x10^5$ cells/well into the upper chambers of a 24-well Transwell plate with a polyester membrane (pore size, 0.4 $\mu$m; Costar; Corning, Inc.). For the Transwell co-culture assay, both the upper and lower chambers were initially supplemented with DMEM containing 10% FBS. Cells were co-cultured at 37˚C with 5% $CO_2$ for 14 days, and 2 days before TEER measurement, the media in both chambers were replaced with serum-free DMEM. The resistance values of different cell models, including inflammatory and non-inflammatory cell models, as well as their ST3Gal1 knockdown or overexpression cell models, were measured using a resistance meter. The relative TEER values were calculated for each group by comparison with the control.

*FITC-dextran permeability assay*. Subsequently, the permeability of different cell models was studied. Notably, the setup of Transwell inserts used in this permeability assay (other than the addition of FITC-dextran) was consistent with that of the aforementioned protocol for TEER measurement. FITC-dextran (4 kDa; MilliporeSigma) was added to the apical compartment of Transwell inserts, with a final concentration of 1 mg/ml. These cell models were incubated at 37˚C for 2 h. Subsequently, a 100-$\mu$l aliquot was aspirated from the lower chamber, and the fluorescence value was measured using a microplate reader (Bio-Rad Laboratories, Inc.) at an excitation wavelength of 492 nm and an emission wavelength of 520 nm. The relative fluorescence values were calculated for each group by comparison with the control.

*Bioinformatics analysis*. For ST3Gal1 expression analysis, datasets including human normal samples and UC samples (GDS3119) (30), as well as UC lesional and non-lesional samples (GSE107499) were obtained from the Gene Expression Omnibus (GEO) database (https://www.ncbi.nlm.

Table II. Antibodies used for western blotting.

| A, Primary antibodies | | | |
|---|---|---|---|
| Name | Company | Cat. no. | Dilution |
| Rabbit polyclonal IgG to ST3Gal1 | Invitrogen; Thermo Fisher Scientific, Inc. | PA5-42726 | 1:1,000 |
| Rabbit monoclonal IgG to CDX2 | Abcam | ab76541 | 1:1,000 |
| Rabbit monoclonal IgG to p-STAT3 | Abcam | ab76315 | 1:1,000 |
| Mouse monoclonal IgG to MUC2 | Abcam | ab11197 | 1:1,000 |
| Rabbit Polyclonal IgG to TFF3 | Proteintech Group, Inc. | 23277-1-AP | 1:1,000 |
| Rabbit polyclonal IgG to STAT3 | Proteintech Group, Inc. | 10253-2-AP | 1:500 |
| Rabbit polyclonal IgG to α-tubulin | Proteintech Group, Inc. | 11224-1-AP | 1:1,000 |
| B, Secondary antibodies | | | |
| HRP-conjugated Affinipure Goat Anti-Rabbit IgG (H+L) | Proteintech Group, Inc. | SA00001-2 | 1:10,000 |
| HRP-conjugated Affinipure Goat Anti-Mouse IgG (H+L) | Proteintech Group, Inc. | SA00001-1 | 1:10,000 |

CDX2, homeobox protein CDX-2; p-, phosphorylated.

nih.gov/geoprofiles/?term=) and analyzed. To investigate the relationship between ST3Gal1 and the severity score of UC, relevant clinical data were extracted from the GEO dataset GSE92415 (31) for analysis. The GEO dataset GDS3859 (32) was used to analyze changes in the mRNA levels of ST3Gal1 in DSS-treated mice. Additionally, the GEO dataset GSE107499 was used to analyze the expression changes of ST3Gal1, as well as the expression profiles of inflammatory mediators, intestine-associated secretory proteins and signaling pathway-related proteins in lesional and non-lesional tissues of UC. Furthermore, the relationships among these factors and proteins in the GSE107499 dataset, specifically within the lesional tissues of UC, were investigated. Dataset processing and statistical analysis were performed using GEO2R (https://www.ncbi.nlm.nih.gov/geo/geo2r/), an official GEO tool. In the present study, this tool was specifically utilized to extract and compare the expression levels of pre-specified target genes (including ST3Gal1, MUC2, TFF3, CDX2, IL-1β, IL-6, IL-8 and STAT3) between experimental groups (for example, UC lesional mucosa vs. UC non-lesional mucosa, and healthy human colon mucosa vs. UC colon mucosa).

*Statistical analysis*. GraphPad Prism 6.0 software (Dotmatics) was utilized for the graphical representation and statistical evaluation of diverse data obtained during the experiment. Data are presented as box and whisker plots (displaying median and interquartile range), scatter plots or as the mean ± SD from at least three independent replicates, with unpaired two-tailed t-test used for comparisons between two groups and Pearson's correlation test used for assessing linear correlations. In addition, one-way ANOVA with Tukey's HSD post hoc multiple comparisons test was applied for multi-group analyses. $P<0.05$ was considered to indicate a statistically significant difference.

## Results

*ST3Gal1 expression in intestinal mucosa from patients with UC and the mouse DSS-induced colitis model is related to the inflammatory status of colitis*. The present study compared the mRNA levels of ST3Gal1 in normal human colon mucosa and the mucosa from patients with UC obtained from the GDS3119 dataset in the GEO. The mRNA expression levels of ST3Gal1 in the mucosal tissue of individuals diagnosed with UC were significantly higher than those in healthy colon mucosa (derived from healthy control individuals) ($P<0.05$; Fig. 1A). Furthermore, mRNA levels of ST3Gal1 in the inflamed mucosal regions of patients with UC were significantly higher than those observed in normal colon mucosa. Additionally, ST3Gal1 expression levels were significantly higher in inflamed UC intestinal mucosa than in non-inflamed UC intestinal mucosa ($P<0.01$; Fig. 1B). Furthermore, the mRNA expression levels of ST3Gal1 in non-lesional mucosa were significantly lower than those in lesional mucosa (GSE107499; $P<0.01$; Fig. 1C). Additionally, in patients with UC, ST3Gal1 mRNA within the inflamed mucosa exhibited progressive, mostly significant upregulation associated with an increasing modified Mayo score (GSE92415; $P<0.01$; Fig. 1D).

The present study further analyzed the mRNA levels of ST3Gal1 in the mucosa of the DSS-induced mouse colitis model. The obtained ST3Gal1 mRNA levels were classified into four groups based on DSS usage: The normal group, classified as mRNA levels obtained prior to DSS administration, and those obtained 2, 4 and 6 days after DSS feeding. ST3Gal1 mRNA expression in the mucosa of mice 6 days after DSS feeding was significantly higher than that in all other groups analyzed (GDS3859; $P<0.01$; Fig. 1E).

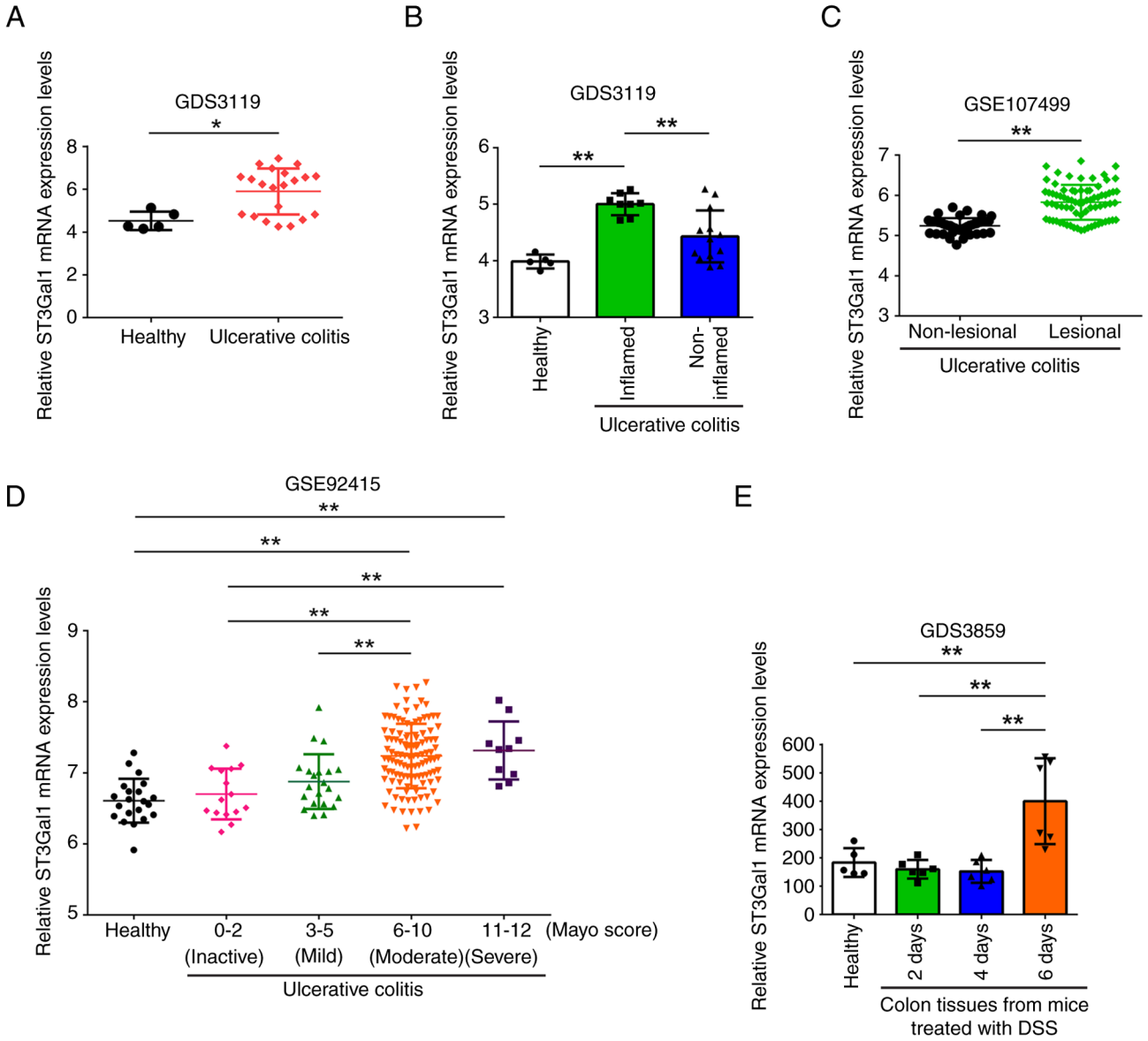


Figure 1. ST3Gal1 mRNA levels in intestinal mucosa from patients with UC and a mouse DSS-induced colitis model are associated with inflammatory states. (A) Comparison of ST3Gal1 mRNA levels between human normal colon mucosa from healthy controls (n=5) and colonic mucosa from patients diagnosed with UC (n=21) in the GDS3119 dataset from the GEO database. (B) ST3Gal1 mRNA levels in human normal colonic tissues from healthy controls (n=5), inflamed colonic tissues from patients with UC and visible macroscopic inflammation (n=8), and non-inflamed colonic mucosal tissues from patients with UC without macroscopic signs of inflammation (n=13) in the GEO dataset GDS3119. (C) ST3Gal1 mRNA levels in non-lesional mucosa (n=44) and lesional mucosa (n=75) from different patients with UC, obtained from the GEO dataset GSE107499. (D) ST3Gal1 mRNA levels in the normal mucosa (n=21) from healthy controls and the inflamed mucosa (n=162) from patients with UC with varying modified Mayo scores in the GEO dataset GSE92415. (E) ST3Gal1 mRNA levels in colon tissues from mice treated with DSS to induce colitis (independent, non-overlapping mice) divided into four groups: Before DSS administration (n=5), and at 2, 4 and 6 days post-DSS treatment (n=6/group). Data were obtained from the GEO dataset GDS3859. Data in A, C and D are presented as box and whisker plots, whereas data in B and E are presented as the mean ± SD. Statistical significance was determined using specific tests for each subpart based on group comparisons: (A and C) Unpaired t-test and (B, D and E) one-way analysis of variance followed by Tukey's post-hoc test. $^{*}$P<0.05 and $^{**}$P<0.01. DSS, dextran sulfate sodium; GEO, Gene Expression Omnibus; UC, ulcerative colitis.

*Establishment of an IEC monolayer and ST3Gal1-knockdown or ST3Gal1-OE models*. The present study first prepared an IEC monolayer model through a co-culture of three distinct cell types, and then obtained ST3Gal1-knockdown and ST3Gal1-OE IEC monolayer cell models using either an ADV1(U6/CMV-GFP) vector and an ST3Gal1 interference sequence insert or a ST3Gal1-OE lentiviral vector. The third interference sequence (ST3Gal1-sh3) had the most efficient inhibitory effect on ST3Gal1 expression in the IEC monolayer model, named ST3Gal1-sh3/IEC for further experiments (P<0.01; Fig. 2A and C). A ST3Gal1-OE assay showed that the ST3Gal1-OE group exhibited a significant increase in ST3Gal1 expression at both mRNA and protein levels in the IEC monolayer model compared with those in the untreated and overexpression control groups (P<0.01; Fig. 2B and D). This model was designated ST3Gal-OE/IEC for further experiments.

The present study used IEC monolayer models to replicate both healthy and inflamed states of the human intestine. To establish an inflamed IEC monolayer model, the

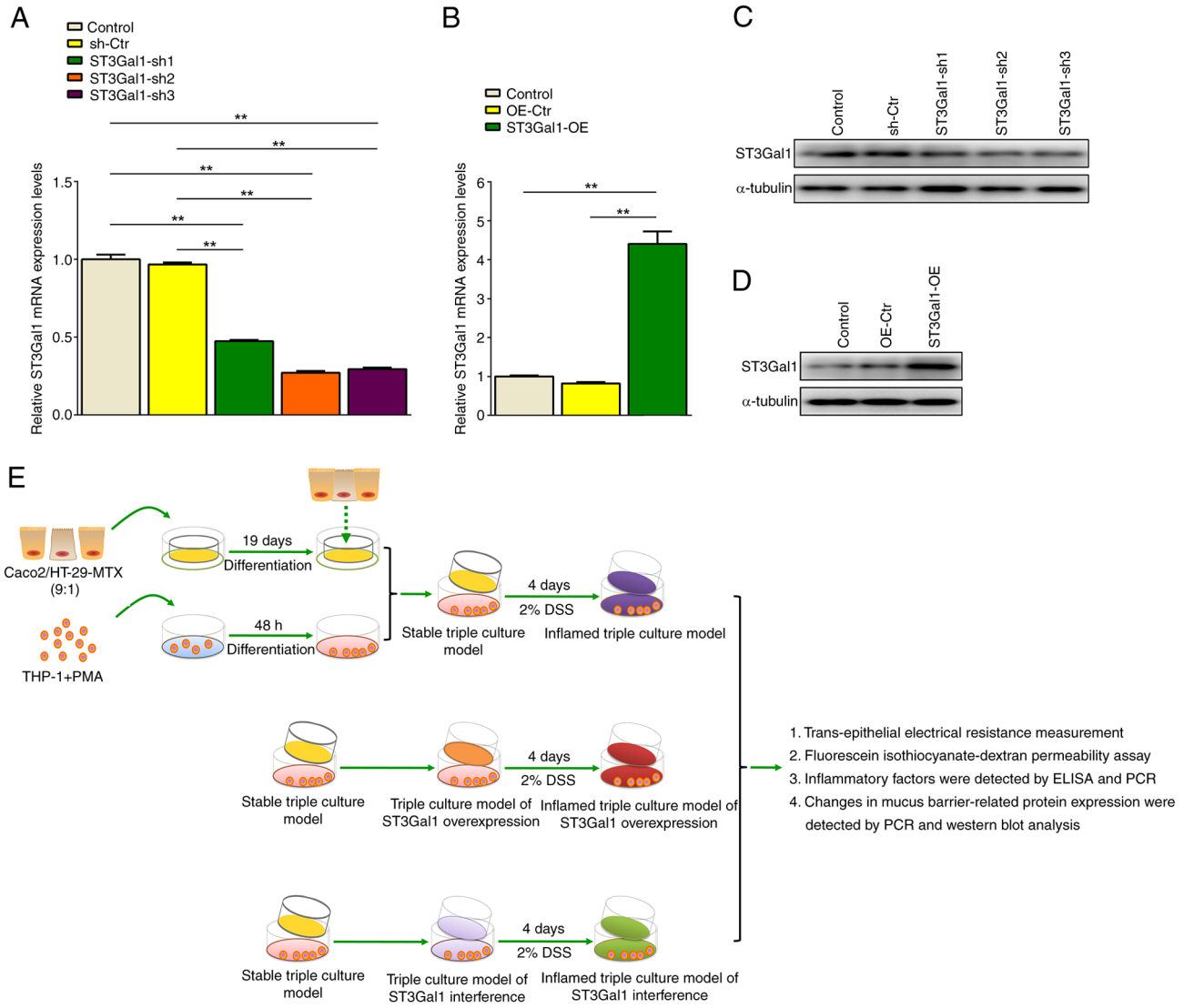


Figure 2. Establishment of ST3Gal1-interfered IEC and ST3Gal1-overexpressed IEC models, and the schematic representation of IEC monolayer grouping. (A) ST3Gal1 mRNA levels in IEC, sh-Ctr/IEC and ST3Gal1-interfered IEC groups 1-3. (B) ST3Gal1 mRNA levels in IEC, OE-Ctr/IEC and ST3Gal1-OE/IEC groups. (C) ST3Gal1 protein levels in IEC, sh-Ctr/IEC and ST3Gal1-interfered IEC groups. (D) ST3Gal1 protein levels in IEC, OE-Ctr/IEC and ST3Gal1-OE/IEC groups. (E) Establishment of IEC monolayers containing sh-Ctr, ST3Gal1-sh3, OE-Ctr and ST3Gal1-OE. The stable triple culture models were treated with fresh complete medium supplemented with 2% DSS for 4 days to obtain inflamed models. Data are presented as the mean ± SD. Statistical significance was assessed using one-way analysis of variance followed by Tukey's post-hoc test. $^{**}$P<0.01. IEC, intestinal epithelial cell; sh, short hairpin; Ctr, control; OE, overexpression; PMA, phorbol 12-myristate 13-acetate; DSS, dextran sulfate sodium.

aforementioned infection models were administered fresh complete medium enriched with 2% DSS for 4 days. The resulting inflamed IEC monolayer model was employed for investigating intestinal barrier integrity and inflammatory mediator secretion (Fig. 2E).

*ST3Gal1 alters the barrier function of the IEC monolayer.* The IEC monolayer barrier was assessed by measuring TEER. The TEER levels in the ST3Gal1-sh3/IEC group were significantly higher than those in the IEC and sh-Ctr/IEC groups after stimulation with 2% DSS (P<0.01; Fig. 3A). By contrast, no notable differences in the TEER levels were observed among the non-inflamed IEC monolayers of the stable triple culture models without 2% DSS treatment (P>0.05; Fig. 3A). The TEER levels of the inflamed ST3Gal1-OE/IEC group were significantly lower compared with those in the IEC or Ctr/IEC groups (P<0.01; Fig. 3B). By contrast, no notable differences were observed among the non-inflamed IEC monolayers of the stable triple culture models (P>0.05; Fig. 3B). The impact of modifications in ST3Gal1 expression on the permeability of IEC monolayers was measured by performing a trans-epithelial permeability assay using FITC-dextran. The assays demonstrated a notable decrease in the FITC-dextran permeability of the inflamed ST3Gal1-sh3/IEC population compared with that in the IEC and sh-Ctr/IEC groups (P<0.01; Fig. 3C). However, no significant difference was observed among the non-inflamed stable triple culture models (P>0.05; Fig. 3C). Notably, a significant increase in the permeability of the inflamed ST3Gal1-OE/IEC group was noted compared with that in the IEC and Ctr/IEC groups (P<0.01; Fig. 3D). By contrast, the non-inflamed triple culture models did not show any significant differences in permeability (P>0.05; Fig. 3D).

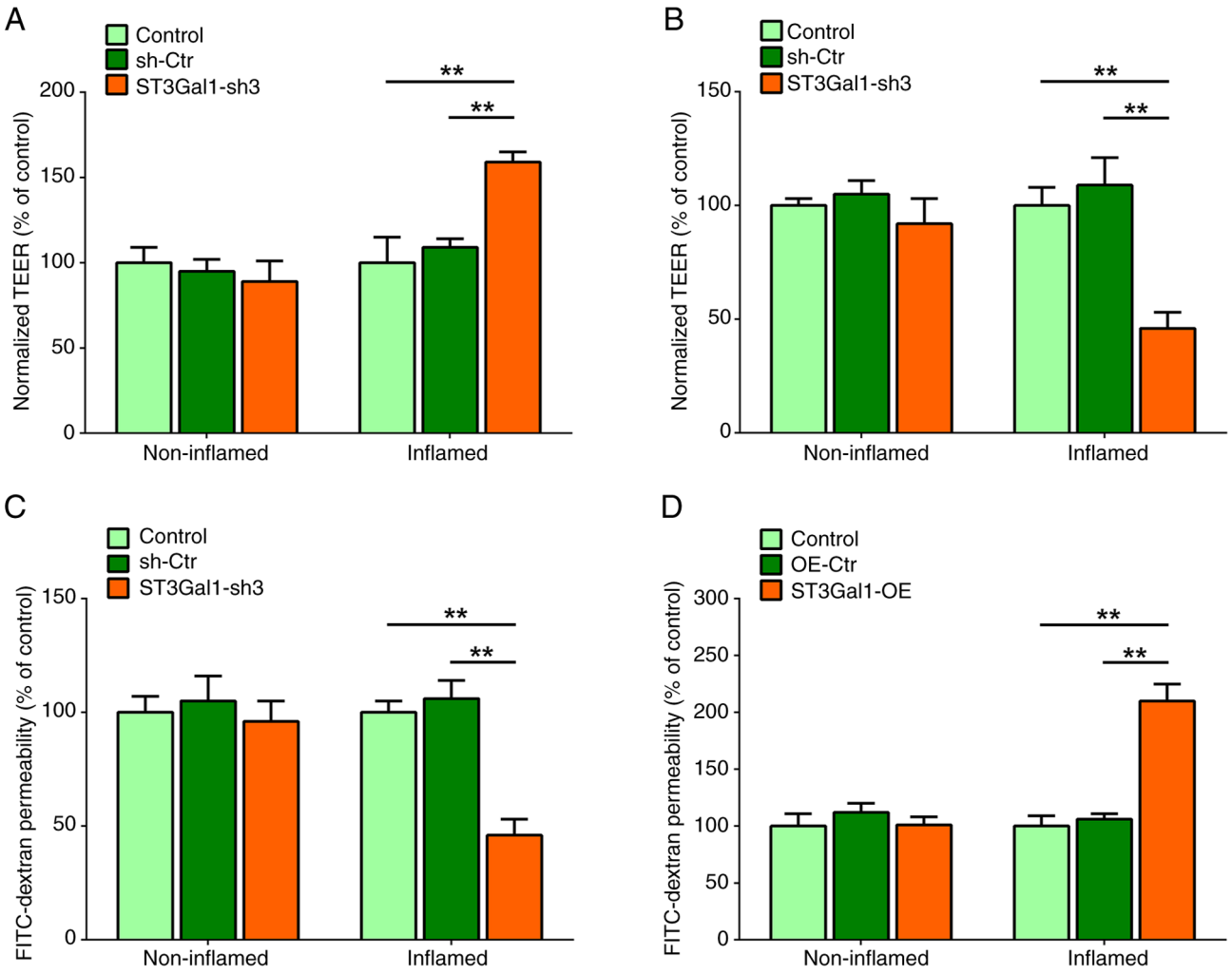


Figure 3. ST3Gal1 expression in triple culture models modulates the epithelial barrier of the IEC monolayers. (A) TEER levels in the IEC monolayers containing sh-Ctr/IEC or ST3Gal1-sh3/IEC with 2% DSS stimulation (inflamed triple culture) or without 2% DSS treatment (non-inflamed triple culture). (B) TEER levels in the inflamed (DSS-treated) and non-inflamed IEC monolayers containing OE-Ctr/IEC or ST3Gal1-OE/IEC. (C) Results of the FITC-dextran permeability assay indicated that there was a significant reduction in the inflamed IEC monolayer containing ST3Gal1-sh3/IEC. (D) There was a significant increase in the permeability of the inflamed IEC monolayer containing ST3Gal1-OE/IEC. Data are presented as the mean ± SD. Statistical significance was assessed using one-way analysis of variance followed by Tukey's post-hoc test. **P<0.01. TEER, trans-epithelial electrical resistance; IEC, intestinal epithelial cell; sh, short hairpin; Ctr, control; OE, overexpression; DSS, dextran sulfate sodium.

Therefore, it may be suggested that ST3Gal1 interference in IECs enhanced the barrier function of the IEC monolayer. However, enforced expression of the ST3Gal1 gene in IECs damaged the barrier function of the IEC monolayer.

*ST3Gal1 expression in the IEC monolayer alters MUC2, TFF3 and CDX2 expression, as well as STAT3 phosphorylation.* Owing to alterations in the intestinal epithelial barrier caused by altered ST3Gal1 expression in the IEC monolayer, the present study detected intestinal mucus barrier-associated MUC2 and TFF3, goblet cell differentiation-associated CDX2 expression and inflammation-associated STAT3 phosphorylation in IEC monolayers. The present study found that ST3Gal1 knockdown in IECs significantly increased the mRNA levels of MUC2, TFF3 and CDX2, but significantly decreased the mRNA levels of STAT3 in the inflamed stable triple culture model compared with those in the control groups (P<0.01; Fig. 4A-D). No significant differences in MUC2, TFF3, CDX2 and STAT3 mRNA levels were observed among the non-inflamed stable triple culture models (P>0.05; Fig. 4A-D). Overexpression of ST3Gal1 in IECs significantly reduced the mRNA levels of MUC2, TFF3 and CDX2 in the inflamed stable triple culture model compared with those in the control groups (P<0.05 or P<0.01; Fig. 4E-H), and the mRNA expression levels of STAT3 were decreased in the inflamed stable triple culture model compared with those in the control groups (P<0.05; Fig. 4H); however, no significant difference was observed when compared with the OE-Ctr group (P>0.05; Fig. 4H). No significant differences were observed in the mRNA levels of MUC2, TFF3, CDX2 and STAT3 among the non-inflamed stable triple-culture models (P>0.05; Fig. 4E-H).

The present study also detected the protein expression levels of MUC2, TFF3, CDX2, phosphorylated (p)-STAT3 and STAT3 in both the inflamed and non-inflamed stable triple culture models. In the inflamed stable triple culture model comprising ST3Gal1-sh3/IEC, the protein levels of MUC2, TFF3 and CDX2 were increased, whereas p-STAT3 levels were notably decreased compared with those in the control

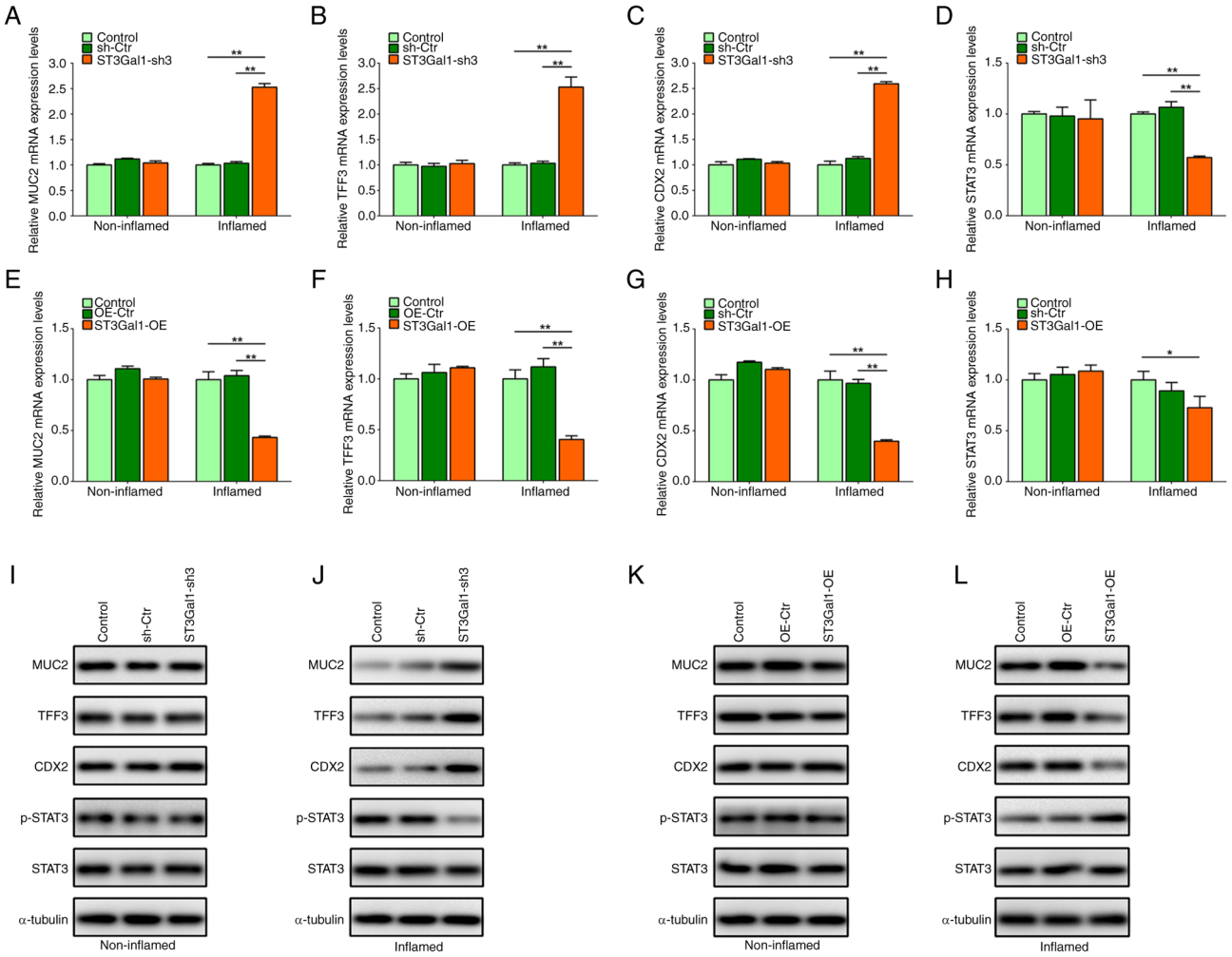


Figure 4. ST3Gal1 expression in inflamed IEC monolayers alters MUC2, TFF3, CDX2, STAT3 and p-STAT3 expression. ST3Gal1 knockdown in ST3Gal1-sh3/IEC significantly increased (A) MUC2, (B) TFF3 and (C) CDX2, but significantly reduced (D) STAT3 mRNA levels in the inflamed IEC monolayer. ST3Gal1 OE in ST3Gal1-OE/IEC significantly reduced (E) MUC2, (F) TFF3 and (G) CDX2 mRNA levels in the inflamed IEC monolayer. (H) ST3Gal1 OE in ST3Gal1-OE/IEC slightly decreased STAT3 mRNA levels in the inflamed IEC monolayer. (I) Western blotting showed no changes in protein expression in non-inflamed knockdown samples. (J) Western blotting showed that MUC2, TFF3 and CDX2 protein levels were increased, and p-STAT3 expression was decreased in the inflamed IEC monolayer comprising ST3Gal1-sh3/IEC. (K) Western blotting showed no notable changes in protein expression in non-inflamed OE samples. (L) Western blotting showed that MUC2, TFF3 and CDX2 protein levels were decreased, and p-STAT3 expression was increased in the inflamed IEC monolayer comprising ST3Gal1-OE/IEC. Data are presented as the mean ± SD. Statistical significance was assessed using one-way analysis of variance followed by Tukey's post-hoc test. $^{*}$P<0.05 and $^{**}$P<0.01. IEC, intestinal epithelial cell; sh, short hairpin; Ctr, control; OE, overexpression; MUC2, mucin 2; TFF3, trefoil factor 3; CDX2, homeobox protein CDX-2; p-, phosphorylated.

groups (Fig. 4J). However, no notable difference was noted in the MUC2, TFF3, CDX2, STAT3 and p-STAT3 protein levels of the non-inflamed stable triple culture models (Fig. 4I). Additionally, the protein levels of MUC2, TFF3 and CDX2 were notably decreased in the inflamed stable triple culture model comprising ST3Gal1-OE/IEC, whereas p-STAT3 levels were increased compared with those in the control groups (Fig. 4L). However, there were no marked differences observed in the MUC2, TFF3, CDX2, STAT3 and p-STAT3 protein levels of the non-inflamed stable triple culture overexpression model (Fig. 4K).

*ST3Gal1 expression is correlated with TFF3 and CDX2 mRNA levels in lesional mucosa obtained from patients with UC*. To support the relationship between ST3Gal1 expression and MUC2, TFF3 and CDX2 mRNA levels in patients with UC, the expression dataset GSE107499 was downloaded, and the mRNA levels of TFF3 and CDX2 in the non-lesional and lesional mucosa from patients with UC, as well as their correlations with ST3Gal1 mRNA expression, were subsequently compared. As illustrated in Fig. 5A, the mRNA expression levels of MUC2 in the affected lesional mucosal tissue were significantly elevated compared with those in the non-lesional mucosa (P<0.05). By contrast, the TFF3 mRNA levels in the lesional mucosa showed no significant difference when compared with those in the non-lesional mucosa of patients with UC (P>0.05; Fig. 5B). Notably, the mRNA levels of CDX2 in the lesional mucosa were significantly lower than those in non-lesional mucosa (P<0.01; Fig. 5C). The correlation analysis revealed that the mRNA expression levels of ST3Gal1 in the lesional mucosal tissue exhibited a negative correlation with the mRNA levels of TFF3 (R=-0.4883; P<0.0001; Fig. 5E) and CDX2 (R=-0.4797; P<0.0001; Fig. 5F) in patients diagnosed with UC. However, no notable correlation was observed

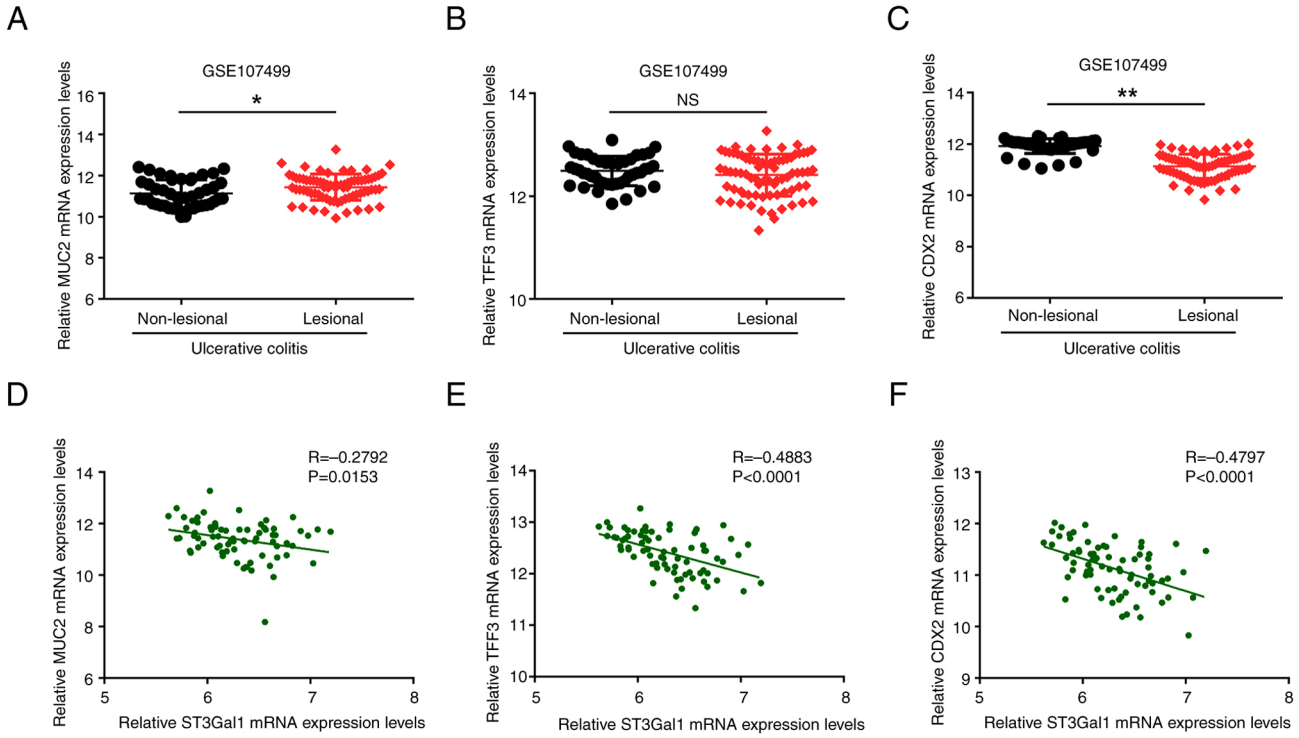


Figure 5. Comparison of (A) MUC2, (B) TFF3 and (C) CDX2 mRNA levels between non-lesional mucosa (n=44) and lesional mucosa (n=75) from distinct patients with ulcerative colitis. Correlations between (D) MUC2, (E) TFF3 and (F) CDX2 mRNA levels and ST3Gal1 expression. Data in A-C are presented as box and whisker plots, and those in D-F as scatter plots. Statistical significance for group comparisons in A-C was assessed using unpaired t-test. Correlation analyses in D-F were performed using Pearson's correlation coefficient. $^{*}$P<0.05 and $^{**}$P<0.01. Data were obtained from the GSE107499 dataset from the Gene Expression Omnibus database. $^{*}$P<0.05 and $^{**}$P<0.01. NS, not significant; MUC2, mucin 2; TFF3, trefoil factor 3; CDX2, homeobox protein CDX-2.

between ST3Gal1 and of MUC2 expression in lesional tissues of patients with UC (R=-0.2792; P<0.05; Fig. 5D).

*ST3Gal1 expression in the IEC monolayer alters the expression of inflammatory mediators*. Supernatants from the inflamed and non-inflamed stable triple culture models comprising ST3Gal1-sh3/IEC and ST3Gal1-OE/IEC were collected to detect the levels of inflammatory mediators. The protein concentrations of inflammatory mediators were quantified via ELISA, whereas the mRNA levels of inflammatory mediators in cell lysates were assessed via RT-qPCR. Notably, knockdown of ST3Gal1 significantly reduced the mRNA expression levels of IL-1β, IL-6 and IL-8 in the inflamed intestinal IEC monolayer, compared with that in the control groups (P<0.01; Fig. 6A-C). This analysis, however, revealed no significant differences in the mRNA levels of IL-1β, IL-6 and IL-8 among the non-inflamed IEC monolayers (P>0.05; Fig. 6A-C). However, the overexpression of ST3Gal1 in ST3Gal1-OE/IEC cells significantly elevated the mRNA levels of IL-1β, IL-6 and IL-8 within the inflamed IEC monolayer compared with the control groups (P<0.01; Fig. 6D-F). By contrast, the non-inflamed IEC monolayer exhibited no significant differences in the expression of these cytokines (P>0.05; Fig. 6D-F). Additionally, a significant decrease in the protein concentrations of IL-1β (720.51±61.01 pg/ml), IL-6 (461.20±98.06 pg/ml) and IL-8 (4,325.37±579.25 pg/ml) was observed in supernatants derived from the inflamed IEC monolayer containing ST3Gal1-sh3/IEC when compared with the control groups (P<0.01; Fig. 6G-I). No significant differences were noted in the protein concentrations of IL-1β (318.43±24.54 pg/ml), IL-6 (404.52±20.55 pg/ml) and IL-8 (3,151.23±156.78 pg/ml) in ST3Gal1-sh3/IEC compared with in the control groups in the supernatants obtained from the non-inflamed IEC monolayer (P>0.05; Fig. 6G-I). In addition, the protein concentrations of IL-1β (1,863.41±62.25 pg/ml), IL-6 (1,797.57±94.93 pg/ml) and IL-8 (18,319.25±1,893.01 pg/ml) were significantly higher in the supernatants derived from the inflamed IEC monolayer containing ST3Gal1-OE/IEC compared with those from the control groups (P<0.01; Fig. 6J-L). Consistent with previous observations in the present study, there were no significant differences in the concentrations of IL-1β (282.01±48.33 pg/ml), IL-6 (408.14±28.22 pg/ml) and IL-8 (4,203.54±433.62 pg/ml) the aforementioned cytokines in the supernatants obtained from the non-inflamed IEC monolayer (P>0.05; Fig. 6J-L). Therefore, it may be inferred that the expression of ST3Gal1 in IECs markedly modified the expression, and subsequent release of IL-1β, IL-6 and IL-8 in inflamed triple culture models.

*ST3Gal1 levels are correlated with IL-1β, IL-6, IL-8 and STAT3 mRNA levels in lesional mucosa obtained from patients with UC*. The present study conducted a comparative analysis of the mRNA expression levels of IL-1β, IL-6, IL-8 and STAT3 between the non-lesional and lesional mucosal tissues of patients diagnosed with UC, which was obtained from the GSE107499 dataset, alongside the relationships of cytokine expression with ST3Gal1 mRNA expression levels. The present results demonstrated that the mRNA levels of IL-1β (P<0.01; Fig. 7A), IL-6 (P<0.01; Fig. 7B), IL-8 (P<0.01; Fig. 7C) and STAT3 (P<0.01; Fig. 7D) in the lesional mucosa were

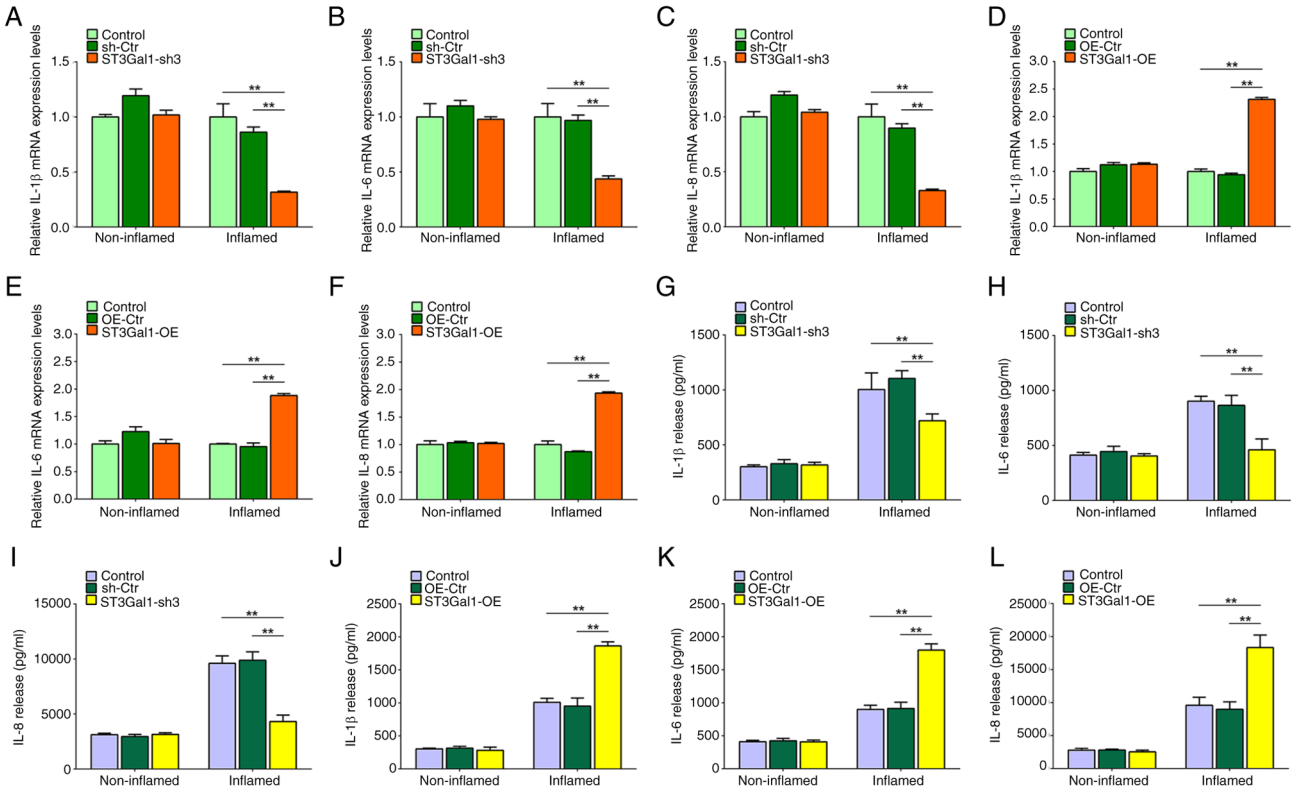


Figure 6. ST3Gal1 expression in the IEC monolayer alters the levels of inflammatory mediators. ST3Gal1 knockdown in ST3Gal1-sh3/IEC significantly reduced the mRNA levels of the inflammatory mediators (A) IL-1β, (B) IL-6 and (C) IL-8 from the inflamed IEC monolayer supernatant. ST3Gal1 OE in ST3Gal1-OE/IEC significantly increased the mRNA levels of the inflammatory mediators (D) IL-1β, (E) IL-6 and (F) IL-8 in the supernatant of the inflamed IEC monolayer. Protein levels of the inflammatory mediators (G) IL-1β, (H) IL-6 and (I) IL-8 were decreased in the supernatant of inflamed ST3Gal1-sh3/IEC. Protein levels of the inflammatory mediators (J) IL-1β, (K) IL-6 and (L) IL-8 were increased in the supernatant of inflamed ST3Gal1-OE/IEC. Data are presented as the mean ± SD, and statistical significance was assessed using one-way ANOVA followed by Tukey's post-hoc test. $^{**}$P<0.01. IEC, intestinal epithelial cell; sh, short hairpin; Ctr, control; OE, overexpression.

significantly elevated compared with those in the non-lesional mucosa. Furthermore, correlation analyses revealed positive correlations between ST3Gal1 mRNA expression and the expression levels of the cytokines IL-1β (R=0.5675; P<0.0001; Fig. 7D), IL-6 (R=0.4117; P=0.0002; Fig. 7E), IL-8 (R=0.5765; P<0.0001; Fig. 7F) and STAT3 (R=0.4079; P=0.0003; Fig. 7H) in the lesional mucosa of patients with UC.

## Discussion

The results of the present study indicated a strong relationship between ST3Gal1 expression in the intestinal epithelium and the barrier function of IECs, as well as with the secretion of inflammatory mediators within the context of intestinal inflammation. ST3Gal1 knockdown in the IEC monolayer increased the barrier function, whereas its overexpression resulted in intestinal barrier function deterioration. Overexpression of ST3Gal1 in the IEC monolayer reduced the expression of intestinal mucus barrier-associated MUC2, TFF3 and CDX2, as well as the expression of inflammation-associated p-STAT3. By contrast, overexpression of ST3Gal1 elevated the levels of inflammatory mediators (IL-1β, IL-6, and IL-8), which are important for maintaining intestinal mucosa homeostasis (33). The DSS-induced colitis model is linked to the inflammatory status of the colonic tissue, as evidenced by the dynamic association between disease progression and the expression profiles of key molecules: Specifically, inflammatory factors (IL-1β, IL-6, IL-8), goblet cell secretory proteins (MUC2, TFF3) and signaling pathway-related proteins (STAT3, p-STAT3). This is supported by the bioinformatics analysis of the GEO dataset GDS3859, where ST3Gal1 mRNA expression in mouse colonic mucosa was significantly upregulated with prolonged DSS treatment (peaking at 6 days post-administration), concurrent with the exacerbation of colonic inflammation. Additionally, in the *in vitro* inflamed triple-culture model induced by 2% DSS, the expression patterns of the aforementioned molecules were consistently altered in response to ST3Gal1 knockdown or overexpression, further confirming that the DSS-induced model recapitulates the intrinsic association between colonic inflammatory status and the expression of these functional proteins in UC. ST3Gal1 facilitates the formation of α2,3-sialic acid residues and contributes to the modification of glycan ends on proteins that possess α2,3-sialic acid residues (34). Dysregulation of ST3Gal1 within IECs can result in the abnormal expression of sialic acid, which is a unique carbohydrate that anchors glycoproteins and glycolipids to the cell membrane through α2,3-sialic acid residue modifications (35). The present study elucidated the role of ST3Gal1 in various IEC monolayers, including inflamed and non-inflamed states, to identify knowledge gaps, and explore its potential application as a novel diagnostic and therapeutic target.

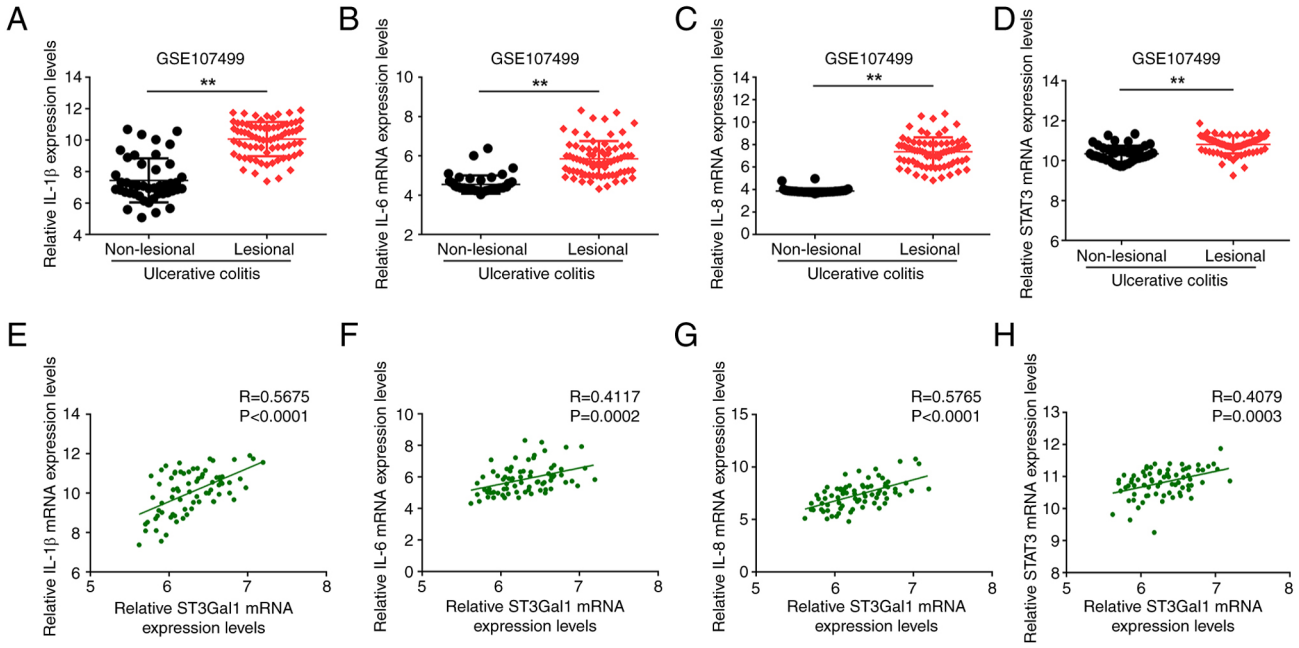


Figure 7. Comparison of the expression of inflammatory mediators (A) IL-1β, (B) IL-6 and (C) IL-8, as well as (D) STAT3 between non-lesional mucosa (n=44) and lesional mucosa (n=75) from distinct patients with ulcerative colitis. Correlations between (E) IL-1β, (F) IL-6, (G) IL-8 and (H) STAT3 mRNA levels and ST3Gal1 expression. Data were obtained from the GSE107499 dataset from the Gene Expression Omnibus database. Data in A-D are presented as box and whisker plots, and those in E-H as scatter plots. Statistical significance for group comparisons in A-D was assessed using the unpaired t-test; correlation analyses in E-H were performed via Pearson's correlation coefficient. $^{**}$P<0.01.

Sialyltransferases are key enzymes in the regulatory mechanisms of various life processes, including cell signaling, cellular recognition, interactions between cells and pathogens, and cancer metastasis (36-38). Among these enzymes, the ST3Gal family stands out as one of the most important enzyme families, comprising six distinct members in both mice and humans: ST3Gal1-6 (39). The ST3Gal family catalyzes the synthesis and attachment of α2,3-linked sialic acid residues to the terminal galactose residues of glycans in proteins through a process known as sialylation. The evolution of distinct human ST3Gal family members, which establish specific α2,3-linkages, suggests a degree of functional specialization; however, the roles of α2,3-linkage in health and disease remain insufficiently investigated (39). Prior research has documented increased sialylation in IBD, as well as in other autoimmune conditions and instances of acute inflammation (40). Notably, α2,6- and α2,3-sialylation of glycans with extensively branched structures appear to escalate during inflammatory responses in CD and UC, respectively, which are mediated by α2,6-sialyltransferases and α2,3-sialyltransferases (41,42). Similarly, ST6 mutations in animal models have been shown to cause impairment of the intestinal mucus barrier, dysbiosis of the intestinal microbiota and increased susceptibility to intestinal inflammation (11,43). Therefore, it can be suggested that ST6 is important for inhibiting bacterial translocation and mitigating inflammation within the intestinal mucus barrier (44). Consequently, the role of α2,3-linkage, catalyzed by ST3Gal1 sialyltransferases, in the pathogenesis of patients with IBD and its underlying mechanisms remain largely unexplored.

IBD refers to a persistent inflammatory disorder affecting the intestines, which is influenced by a combination of genetic predispositions, immune responses and environmental elements (45). To facilitate research on IBD, 66 distinct animal models have been developed at present, which can be classified into chemical treatment models, cell migration models, gene mutation models and gene transfer models (46). However, in some mouse models with few IBD-related genes, the specific pathogenic mechanisms of IBD are more complex than previously predicted (46). To investigate the pathogenic mechanisms and therapeutic approaches of IBD under healthy conditions and inflammatory microenvironments, respectively, researchers have established tri-culture cell models of healthy and inflamed states *in vitro*. Based on these models, various complex *in vitro* culture systems and derivative systems have been developed, including primary cell organoid culture systems, multicellular co-culture systems and chip device systems (24,47,48). The present study established an *in vitro* intestinal barrier simulation model by co-culturing three cell lines: i) HT29-MTX-E12 cells, which exhibit goblet cell characteristics and have a mucus-secreting ability, can be used to simulate the intestinal mucus layer *in vitro*; ii) Caco-2 cells with epithelial cell properties, which were seeded in the upper layer; and iii) differentiable THP-1 inflammatory cells, which were seeded in the basal side. Subsequently, this model was treated with 2% DSS to induce an inflammatory state. The effect of ST3Gal on the integrity of the IEC monolayer barrier was then evaluated by measuring TEER and FITC-dextran permeability. Additionally, as reported in previous studies, the secretion levels of relevant inflammatory factors and the expression of intestinal barrier-related proteins were compared between inflammatory and non-inflammatory states (49-51). The tri-culture system designed to simulate intestinal conditions streamlined the present model, enhancing its robustness and reproducibility (24). The epithelial Transwell cultures

incorporating Caco-2 and HT29-MTX-E12 cell lines exhibited traits that closely resemble those of human intestinal mucosal epithelium. Furthermore, the inclusion of immune-competent THP-1 cells contributed to the immune mechanisms associated with the development of IBD (21). Notably, both the presence of these immune effector cells and the persistence of inflammatory processes substantially influenced the sensitivity of the IEC monolayer.

However, there remains a lack of α2,3-sialylation-linked target molecules bridging ST3Gal1 and intestinal mucus barrier-associated MUC2, TFF3 and CDX2, as well as inflammation-associated molecules, such as IL-1β, IL-6, IL-8, STAT3 and p-STAT3. Further study is required to identify ST3Gal1-mediated molecules with post-translation α2,3-sialylation at their glycan termini. This may help identify novel target molecules to modulate the intestinal epithelial barrier function important for the pathogenesis of human IBD.

The present study provided a new direction for the treatment of UC and other IBDs and showed that ST3Gal1 can act as a potential therapeutic target. Overexpression of ST3Gal1 was directly associated with impaired intestinal barrier function, elevated expression of the pro-inflammatory cytokines IL-1β, IL-6 and IL-8, and increased disease activity in patients with UC, supported by *in vitro* and clinical data: i) *In vitro*, ST3Gal1 overexpression in the inflamed triple-culture model showed significantly reduced TEER, increased FITC-dextran permeability, downregulated expression of barrier-protective proteins MUC2, TFF3 and CDX2, and upregulated p-STAT3, as well as elevated mRNA and protein levels of IL-1β, IL-6 and IL-8. ii) Clinically, bioinformatics analysis of GEO datasets (GSE107499 and GSE92415) revealed that ST3Gal1 mRNA expression was significantly higher in lesional vs. non-lesional mucosa inpatients with UC, it was positively associated with modified Mayo scores (a measure of UC disease activity), and it was positively correlated with the mRNA levels of IL-1β, IL-6, IL-8 and STAT3 in UC lesional tissues. By contrast, ST3Gal1 knockdown upregulated the barrier-protective molecules (MUC2, TFF3 and CDX2) and reduced p-STAT3 expression, thereby repairing the mucosal barrier and alleviating inflammation. Compared with traditional broad-spectrum immunosuppressive therapies, ST3Gal1-targeted interventions may act precisely on the glycosylation pathway, thereby potentially minimizing off-target effects. Additionally, the characteristic high expression of ST3Gal1 in inflamed mucosal tissues enables it to serve as a potential biomarker for assessing disease activity or treatment response. Future studies should validate the efficacy of ST3Gal1 inhibitors in animal models or explore their synergistic effects with existing drugs, such as mesalamine, to provide more precise therapeutic options for IBD.

While the Caco-2/HT29-MTX-E12/THP-1 triple-culture model recapitulated key intestinal mucosal features and followed the 3R principles, it failed to fully replicate the *in vivo* intestinal microenvironment, lacking fibroblasts, endothelial cells and diverse gut microbiota, which are all regulators of mucosal barrier function and IBD inflammation (52). Furthermore, immortalized cell lines such as those used in the present study may not reflect the phenotypes or functions of primary cells of patients with IBD, thus limiting translational relevance.

The clinical analyses of the present study, which relied on retrospective GEO data, also had inherent constraints: i) The lack of access to detailed patient metadata, such as age and treatment history, or long-term paired samples, which would preclude ST3Gal1-prognosis/treatment response analyses; and ii) limited sample sizes of subgroups, such as the UC non-inflamed mucosa group, reduced the power of the correlation analysis for ST3Gal1 with MUC2, which as a key intestinal mucosal barrier component and goblet cell marker, is closely implicated in UC pathogenesis (53). To address these limitations, future studies should: i) Validate the findings of the present study by using primary IEC-organoid models with microbiota or stromal cells for improved physiological relevance; ii) use prospective, well-characterized clinical cohorts to clarify the clinical utility of ST3Gal1; and iii) apply glycoproteomic methods, such as lectin affinity chromatography-mass spectrometry, to identify ST3Gal1-mediated α-2,3-sialylation target molecules to strengthen the mechanistic and translational value of the present results.

In conclusion, the present study provided evidence that ST3Gal1-catalyzed α2,3-linkage formation in IEC may be closely associated with intestinal barrier function. This relationship could be mediated through the distinct influence of ST3Gal1 on the expression of intestinal barrier-associated proteins, including MUC2, TFF3 and CDX2, which are important for preserving the integrity of the intestinal barrier. Additionally, ST3Gal1 modulated the expression of associated inflammatory mediators and transcription factors, including the expression of IL-1β, IL-6, IL-8 and STAT3, which serve important roles in regulating intestinal mucosal inflammation, thereby further linking ST3Gal1 to barrier function.

## Acknowledgements

Not applicable.

## Funding

The present work was supported by the Natural Science Foundation of Chongqing (grant no. cstc2020jcyj-msxmX1094).

## Availability of data and materials

The data generated in the present study may be requested from the corresponding author.

## Authors' contributions

YT, YL, YS, LR and LL were responsible for performing the experiments, and collecting and analyzing the data; specifically, they performed *in vitro* cell culture (triple-culture model establishment, ST3Gal1 overexpression/knockdown), functional assays (TEER, FITC-dextran permeability), molecular experiments (RT-qPCR, western blotting, ELISA), and bioinformatics data processing (GEO dataset analysis). JY substantially contributed to study conception and design, provided critical project oversight (experimental direction, data validation), and led manuscript drafting and critical revision for key intellectual content. RW critically revised the manuscript by interpreting the biological significance

of core findings (for example, linking ST3Gal1-mediated α2,3-sialylation to intestinal barrier dysfunction in UC) and standardizing the academic expression of results (refining data description and mechanistic discussion logic). The manuscript was authored by JY and RW, with JY providing project oversight. JY and YT confirm the authenticity of all the raw data. All authors have read, critically revised, and approved the final manuscript.

**Ethics approval and consent to participate**

Not applicable.

**Patient consent for publication**

Not applicable.

**Competing interests**

The authors declare that they have no competing interests.

**References**


1. Furfaro F, Ragaini E, Peyrin-Biroulet L and Danese S: Novel therapies and approaches to inflammatory bowel disease (IBD). J Clin Med 11: 4374, 2022.
2. Selvakumar B and Samsudin R: Intestinal barrier dysfunction in inflammatory bowel disease: Pathophysiology to precision therapeutics. Inflamm Bowel Dis 31: 450-3464, 2025.
3. Marincola Smith P, Choksi YA, Markham NO, Hanna DN, Zi J, Weaver CJ, Hamaamen JA, Lewis KB, Yang J, Liu Q, *et al*: Colon epithelial cell TGFβ signaling modulates the expression of tight junction proteins and barrier function in mice. Am J Physiol Gastrointest Liver Physiol 320: G936-G957, 2021.
4. Rader AG, Cloherty APM, Patel KS, Almandawi DDA, Perez-Vargas J, Wildenberg ME, Muncan V, Schreurs R, Jean F and Ribeiro CMS: Autophagy-enhancing strategies to promote intestinal viral resistance and mucosal barrier function in SARS-CoV-2 infection. Autophagy Rep 4: 2514232, 2025.
5. Wang R, Xie L, Jiang P, Hou Y, Li D and Wang W: Metformin may improve intestinal mucosal barrier function and help prevent and reverse colorectal cancer in mice. J Cancer 16: 3703-3711, 2025.
6. Esmail S and Manolson MF: Advances in understanding N-glycosylation structure, function, and regulation in health and disease. Eur J Cell Biol 100: 151186, 2021.
7. Montag N, Gousis P and Wittmann J: The emerging role of GlycoRNAs in immune regulation and recognition. Immunol Lett 276: 107048, 2025.
8. Flynn RA, Pedram K, Malaker SA, Batista PJ, Smith BAH, Johnson AG, George BM, Majzoub K, Villalta PW, Carette JE, *et al*: Small RNAs are modified with N-glycans and displayed on the surface of living cells. Cell 188: 4470, 2025.
9. He M, Zhou X and Wang X: Glycosylation: Mechanisms, biological functions and clinical implications. Signal Transduct Target Ther 9: 194, 2024.
10. Wang G, Yuan J, Luo J, Ocansey DKW, Zhang X, Qian H, Xu W and Mao F: Emerging role of protein modification in inflammatory bowel disease. J Zhejiang Univ Sci B 23: 173-188, 2022.
11. Kudelka MR, Stowell SR, Cummings RD and Neish AS: Intestinal epithelial glycosylation in homeostasis and gut microbiota interactions in IBD. Nat Rev Gastroenterol Hepatol 17: 597-617, 2020.
12. Yao Y, Kim G, Shafer S, Chen Z, Kubo S, Ji Y, Luo J, Yang W, Perner SP, Kanellopoulou C, *et al*: Mucus sialylation determines intestinal host-commensal homeostasis. Cell 185: 1172-1188.e28, 2022.
13. Fan Q, Li M, Zhao W, Zhang K, Li M and Li W: Hyper α2,6-Sialylation promotes CD4+ T-Cell activation and induces the occurrence of ulcerative colitis. Adv Sci (Weinh) 10: e2302607, 2023.
14. Shu X, Li J, Chan UI, Su SM, Shi C, Zhang X, An T, Xu J, Mo L, Liu J, *et al*: BRCA1 insufficiency induces a hypersialylated acidic tumor microenvironment that promotes metastasis and immunotherapy resistance. Cancer Res 83: 2614-2633, 2023.
15. Fan TC, Yeo HL, Hung TH, Chang NC, Tang YH, Yu J, Chen SH and Yu AL: ST3GAL1 regulates cancer cell migration through crosstalk between EGFR and neuropilin-1 signaling. J Biol Chem 301: 108368, 2025.
16. Hong Y, Walling BL, Kim HR, Serratelli WS, Lozada JR, Sailer CJ, Amitrano AM, Lim K, Mongre RK, Kim KD, *et al*: ST3GAL1 and βII-spectrin pathways control CAR T cell migration to target tumors. Nat Immunol 24: 1007-1019, 2023.
17. Tajadura-Ortega V, Gambardella G, Skinner A, Halim A, Van Coillie J, Schjoldager KTG, Beatson R, Graham R, Achkova D, Taylor-Papadimitriou J, *et al*: O-linked mucin-type glycosylation regulates the transcriptional programme downstream of EGFR. Glycobiology 31: 200-210, 2021.
18. Zaro BW, Bateman LA and Pratt MR: Robust in-gel fluorescence detection of mucin-type O-linked glycosylation. Bioorg Med Chem Lett 21: 5062-5066, 2011.
19. Zhang Y, Wang L, Ocansey DKW, Wang B, Wang L and Xu Z: Mucin-Type O-Glycans: Barrier, microbiota, and immune anchors in inflammatory bowel disease. J Inflamm Res 14: 5939-5953, 2021.
20. Bergstrom K, Shan X, Casero D, Batushansky A, Lagishetty V, Jacobs JP, Hoover C, Kondo Y, Shao B, Gao L, *et al*: Proximal colon-derived O-glycosylated mucus encapsulates and modulates the microbiota. Science 370: 467-472, 2020.
21. Zhao Z, Zheng W, Zhang L, Song W and Wang T: Sialyltransferase ST3GAL1 promotes malignant progression in glioma. Xi Bao Yu Fen Zi Mian Yi Xue Za Zhi 41: 308-317, 2025 (In Chinese).
22. Busch M, Kämpfer AAM and Schins RPF: An inverted in vitro triple culture model of the healthy and inflamed intestine: Adverse effects of polyethylene particles. Chemosphere 284: 131345, 2021.
23. Busch M, Ramachandran H, Wahle T, Rossi A and Schins RPF: Investigating the role of the NLRP3 inflammasome pathway in acute intestinal inflammation: Use of THP-1 knockout cell lines in an advanced triple culture model. Front Immunol 13: 898039, 2022.
24. Kämpfer AAM, Busch M, Büttner V, Bredeck G, Stahlmecke B, Hellack B, Masson I, Sofranko A, Albrecht C and Schins RPF: Model complexity as determining factor for in vitro nanosafety studies: Effects of silver and titanium dioxide nanomaterials in intestinal models. Small 17: e2004223, 2021.
25. Aske KC and Waugh CA: Expanding the 3R principles: More rigour and transparency in research using animals. EMBO Rep 18: 1490-1492, 2017.
26. Deng X, Shang L, Du M, Yuan L, Xiong L and Xie X: Mechanism underlying the significant role of the miR-4262/SIRT1 axis in children with inflammatory bowel disease. Exp Ther Med 20: 2227-2235, 2020.
27. Samak G, Chaudhry KK, Gangwar R, Narayanan D, Jaggar JH and Rao R: Calcium/Ask1/MKK7/JNK2/c-Src signalling cascade mediates disruption of intestinal epithelial tight junctions by dextran sulfate sodium. Biochem J 465: 503-515, 2015.
28. Pan Q, Tian Y, Li X, Ye J, Liu Y, Song L, Yang Y, Zhu R, He Y, Chen L, *et al*: Enhanced membrane-tethered mucin 3 (MUC3) expression by a tetrameric branched peptide with a conserved TFLK motif inhibits bacteria adherence. J Biol Chem 288: 5407-5416, 2013.
29. Livak KJ and Schmittgen TD: Analysis of relative gene expression data using real-time quantitative PCR and the 2(-Delta Delta C(T)) method. Methods 25: 402-408, 2001.
30. Olsen J, Gerds TA, Seidelin JB, Csillag C, Bjerrum JT, Troelsen JT and Nielsen OH: Diagnosis of ulcerative colitis before onset of inflammation by multivariate modeling of genome-wide gene expression data. Inflamm Bowel Dis 15: 1032-1038, 2009.
31. Sandborn WJ, Feagan BG, Marano C, Zhang H, Strauss R, Johanns J, Adedokun OJ, Guzzo C, Colombel JF, Reinisch W, *et al*: Subcutaneous golimumab induces clinical response and remission in patients with moderate-to-severe ulcerative colitis. Gastroenterology 146: 85-95, 2014.
32. Fang K, Bruce M, Pattillo CB, Zhang S, Stone R II, Clifford J and Kevil CG: Temporal genomewide expression profiling of DSS colitis reveals novel inflammatory and angiogenesis genes similar to ulcerative colitis. Physiol Genomics 43: 43-56, 2011.

33. Xu W, Guo Y, Huang Z, Zhao H, Zhou M, Huang Y, Wen D, Song J, Zhu Z, Sun M, *et al*: Small heat shock protein CRYAB inhibits intestinal mucosal inflammatory responses and protects barrier integrity through suppressing IKKβ activity. Mucosal Immunol 12: 1291-1303, 2019.
34. Fan J, Huang S, Cao C, Jin X and Su Y: The roles of ST3Gal1-6 in cancer: Expression profiles and functional implications. Carbohydr Res 559: 109740, 2025.
35. Ma X, Li M, Wang X, Qi G, Wei L and Zhang D: Sialylation in the gut: From mucosal protection to disease pathogenesis. Carbohydr Polym 343: 122471, 2024.
36. Al Saoud R, Hamrouni A, Idris A, Mousa WK and Abu Izneid T: Recent advances in the development of sialyltransferase inhibitors to control cancer metastasis: A comprehensive review. Biomed Pharmacother 165: 115091, 2023.
37. Perez S, Fu CW and Li WS: Sialyltransferase inhibitors for the treatment of cancer metastasis: Current challenges and future perspectives. Molecules 26: 5673, 2021.
38. Uslupehlivan M, Şener E and İzzetoğlu S: Computational analysis of the structure, glycosylation and CMP binding of human ST3GAL sialyltransferases. Carbohydr Res 486: 107823, 2019.
39. Hatano K, Miyamoto Y, Nonomura N and Kaneda Y: Expression of gangliosides, GD1a, and sialyl paragloboside is regulated by NF-κB-dependent transcriptional control of α2,3-sialyltransferase I, II, and VI in human castration-resistant prostate cancer cells. Int J Cancer 129: 1838-1847, 2011.
40. Kelm M, Quiros M, Azcutia V, Boerner K, Cummings RD, Nusrat A, Brazil JC and Parkos CA: Targeting epithelium-expressed sialyl Lewis glycans improves colonic mucosal wound healing and protects against colitis. JCI Insight 5: e135843, 2020.
41. Taniguchi M, Okumura R, Matsuzaki T, Nakatani A, Sakaki K, Okamoto S, Ishibashi A, Tani H, Horikiri M, Kobayashi N, *et al*: Sialylation shapes mucus architecture inhibiting bacterial invasion in the colon. Mucosal Immunol 16: 624-641, 2023.
42. Zhao T, Liu S, Ma X, Shuai Y, He H, Guo T, Huang W, Wang Q, Liu S, Wang Z, *et al*: Lycium barbarum arabinogalactan alleviates intestinal mucosal damage in mice by restoring intestinal microbes and mucin O-glycans. Carbohydr Polym 330: 121882, 2024.
43. Kotlarz D: Mucus sialylation maintains the peace in intestinal host microbe relations. Gastroenterology 163: 527-528, 2022.
44. Sánchez-Martínez E, Garrido-Romero M and Moreno FJ: Functional role of ST6GALNAC1-mediated sialylation of mucins in preserving intestinal barrier integrity and ameliorating inflammation. Allergy 77: 3697-3698, 2022.
45. Petit C, Rozières A, Boschetti G, Viret C, Faure M, Nancey S and Duclaux-Loras R: Advances in understanding intestinal homeostasis: Lessons from inflammatory bowel disease and monogenic intestinal disorder pathogenesis. Int J Mol Sci 26: 6133, 2025.
46. Mizoguchi A: Animal models of inflammatory bowel disease. Prog Mol Biol Transl Sci 105: 263-320, 2012.
47. Le NPK, Altenburger MJ and Lamy E: Development of an Inflammation-triggered in vitro 'Leaky Gut' Model using Caco-2/HT29-MTX-E12 combined with Macrophage-like THP-1 cells or primary Human-derived macrophages. Int J Mol Sci 24: 7427, 2023.
48. Weber L, Kuck K, Jürgenliemk G, Heilmann J, Lipowicz B and Vissiennon C: Anti-Inflammatory and Barrier-stabilising effects of myrrh, coffee charcoal and chamomile flower Extract in a Co-Culture cell model of the intestinal mucosa. Biomolecules 10: 1033, 2020.
49. Ma L, Zhang X, Zhang C, Hou B and Zhao H: FOSL1 knockdown ameliorates DSS-induced inflammation and barrier damage in ulcerative colitis via MMP13 downregulation. Exp Ther Med 24: 551, 2022.
50. Roselli M, Maruszak A, Grimaldi R, Harthoorn L and Finamore A: Galactooligosaccharide treatment alleviates DSS-induced colonic inflammation in Caco-2 cell model. Front Nutr 9: 862974, 2022.
51. Wang Y, Wen R, Liu D, Zhang C, Wang ZA and Du Y: Exploring effects of chitosan oligosaccharides on the DSS-Induced intestinal barrier impairment in vitro and in vivo. Molecules 26: 2199, 2021.
52. De Cecco F, Franceschelli S, Panella V, Maggi MA, Bisti S, Bravo Nuevo A, D'Ardes D, Cipollone F and Speranza L: Biological response of treatment with saffron petal extract on Cytokine-induced oxidative stress and inflammation in the Caco-2/Human leukemia monocytic Co-Culture model. Antioxidants (Basel) 13: 1257, 2024.
53. Yin S, Yang H, Tao Y, Wei S, Li L, Liu M and Li J: Artesunate ameliorates DSS-induced ulcerative colitis by protecting intestinal barrier and inhibiting inflammatory response. Inflammation 43: 765-776, 2020.